Progress of Theoretical Physics, Vol. 73, No. 2, February 1985

Study of One-Dimensional Quantum Spin Systems by the Transfer-Matrix Method

Hiroshi BETSUYAKU

Japan Atomic Energy Research Institute, Tokai, Ibaraki 319-11

(Received September 25, 1984)

The Suzuki-Trotter formula has been used to get the mth approximant to the classical representation of the partition function of the one-dimensional N-spin $S=\frac{1}{2}$ quantum spin systems. The equivalent two-dimensional $(N\times 2m)$ Ising model with four-spin interactions has been studied in detail by using the numerically exact transfer-matrix method for $T\geqq 0.05$ and $m\leqq 8$. The convergence properties have been examined in two different representations; checkerboard decomposition (CBD) and real-space decomposition (RSD). The spin correlation functions in RSD converge much faster than those in CBD. The limiting $m\to\infty$ behavior has been estimated from the extrapolation formula of the form: $E(m)=E(\infty)+a/m^2$. The limiting values of the energy derived from the nearest-neighbor correlation agree with the correct values excellently.

§ 1. Introduction

In 1976 Suzuki[1] demonstrated that the mth approximant to the classical representation of the partition function of the quantum system described by the Hamiltonian

$$\mathcal{H}=\sum_{l=1}^{k}A_l \tag{1·1}$$

is represented by

$$Z_m=\mathrm{Tr}[\prod_{l=1}^{k}\exp(-\beta A_l/m)]^m, \tag{1·2}$$

on the basis of the generalized Trotter formula.[2] He then proved that a d-dimensional quantum system can be mapped onto a $(d+1)$-dimensional classical Ising system with four-spin interactions. Besides its intrinsic interest, formula (1·2) is very appealing from the viewpoint of numerical studies on quantum statistical mechanics, because it is possible to calculate the thermodynamic properties with the knowledge of only eigenvalues and eigenstates of each A_l without diagonalizing the full Hamiltonian $\mathcal{H}$. Since the pioneering work of Suzuki et al.,[3] several quantum systems have been studied by performing Monte Carlo simulations on the equivalent classical systems.[4),5]

There is no unique classical representation for a given quantum Hamiltonian. Therefore it is necessary to study the convergence properties of different representations by means of exact calculations before one proceeds to Monte Carlo simulations on more complicated quantum systems. The aim of the present article is to point out that the numerically exact transfer-matrix method[6),7] provides a very promising means for such calculations. The convergence properties are examined in two different representations; checkerboard decompositon (CBD) and real-space decomposition (RSD). It is shown that the spin correlation functions in RSD converge much faster than those in CBD.

The present article reports the result applied to the one-dimensional $(1D)S=\frac{1}{2}$

quantum spin system described by the Hamiltonian:

$$\mathcal{H}=-2\sum_{i=1}^{N-1}(J_x S_i^x S_{i+1}^x+J_y S_i^y S_{i+1}^y+J_z S_i^z S_{i+1}^z) \tag{1·3a}$$

$$\equiv\sum_{i=1}^{N-1} V_i\,, \tag{1·3b}$$

where S_i^α is the spin operator on site i and N is the number of spins. We confine ourselves to the following three cases: (1) the ferromagnetic isotropic Heisenberg model

$$J_x=J_y=J_z=J\,; \tag{1·4}$$

(2) the antiferromagnetic isotropic Heisenberg model

$$J_x=J_y=J_z=-J; \tag{1·5}$$

and (3) the XY model

$$J_x=J_y=J\,,\qquad J_z=0\,. \tag{1·6}$$

Over the years various results have been obtained for those models with the use of a wide variety of methods, both exact and approximate. The energy, specific heat, and susceptibility of the 1D ferromagnetic and antiferromagnetic Heisenberg models were estimated by Bonner and Fisher.[8] They used numerical method to diagonalize the full Hamiltonian for finite-size rings and chains, and extrapolated these results to the infinite systems. The present approach which diagonalizes only the local Hamiltonian A_l gives a very useful extrapolation scheme complementary to their finite-size extrapolation; the results extrapolated from finite Trotter size of m for effectively infinite chains are as exact as those extrapolated from finite-size rings and chains. The 1D XY model was solved analytically by Lieb et al.[9] and by Katsura,[10] independently. The preliminary result applied to this model has been reported earlier;[11] the limiting value of the energy obtained by the present method agrees with the exact solution except at extremely low temperatures.

The CBD representation is reviewed in §2 which gives the starting formulation of the numerically exact transfer-matrix method. In §3 the procedure for computation is given in detail. In §4 the results for energy and specific heat calculated in CBD are presented in conjunction with certain exact and/or accurate numerical results. The results are also compared with Monte Carlo simulations. The RSD representation is reviewed in §5 and a proof is given for the equivalence of the thermodynamic properties in CBD and RSD. In §6 the results for the energy derived from the spin correlation functions are presented and the limiting $m\to\infty$ behavior is examined. Summary and conclusions are given in §7.

§ 2. The CBD representation

The simplest classical representation is the checkerboard decomposition (CBD) introduced by Barma and Shastry.[12] It decomposes the Hamiltonian into two parts:

$$\mathcal{H}=A_1+A_2;\quad A_1=\sum_{i\in A} V_i,\quad A_2=\sum_{i\in B} V_i\,, \tag{2·1}$$

where $A(B)$ is the set of odd (even) integers. Substituting this into Eq. (1·2) and

inserting $2m$ complete set of eigenstates of the Ising part of $\mathcal{H}$, the classical representation of the partition function Z_m^{CBD} is given by

$$Z_m^{\mathrm{CBD}}=\sum_{\alpha_1\alpha_2\cdots\alpha_{2m}}\langle\alpha_1|e^{-\beta A_1/m}|\alpha_2\rangle\langle\alpha_2|e^{-\beta A_2/m}|\alpha_3\rangle\cdots\langle\alpha_{2m}|e^{-\beta A_2/m}|\alpha_1\rangle, \tag{2·2}$$

where the states $|\alpha_r\rangle$ are obtained by prescribing the eigenstates of S_i^z for all i. Thus

$$S_i^z|\alpha_r\rangle=S_{ir}|\alpha_r\rangle \quad , \quad \left(S_{ir}=\pm\frac{1}{2}\right) \tag{2·3}$$

where r is a label along the new Trotter direction, and each α_r runs over 2^N states. Each of A_1 and A_2 is the sum of commuting terms in this decomposition, which makes the calculation of the partition function much easier. Equation (2·2) is then rewritten as

$$Z_m^{\mathrm{CBD}}=\sum_{\alpha_1\alpha_2\cdots\alpha_{2m}}\exp\left[-\beta\sum_{i\in A}\sum_{r\in A'}\hat{\mathcal{H}}(i,r)-\beta\sum_{i\in B}\sum_{r\in B'}\hat{\mathcal{H}}(i,r)\right], \tag{2·4}$$

where

$$\exp[-\beta\hat{\mathcal{H}}(i,r)]=\langle S_{ir}S_{i+1r}|\exp(-\beta V_i/m)|S_{ir+1}S_{i+1r+1}\rangle \tag{2·5}$$

with $A'(B')$ being the set of odd (even) r. The matrix $\hat{\mathcal{O}}\equiv\exp(-\beta V_i/m)$ has eight nonzero elements, and these are, in a self-evident notation, as follows:[1),12)]

$$\begin{aligned}
&\langle\uparrow\uparrow|\hat{\mathcal{O}}|\uparrow\uparrow\rangle=\langle\downarrow\downarrow|\hat{\mathcal{O}}|\downarrow\downarrow\rangle=e^{K_z}\cosh K_-\,,\\
&\langle\uparrow\downarrow|\hat{\mathcal{O}}|\uparrow\downarrow\rangle=\langle\downarrow\uparrow|\hat{\mathcal{O}}|\downarrow\uparrow\rangle=e^{-K_z}\cosh K_+\,,\\
&\langle\uparrow\downarrow|\hat{\mathcal{O}}|\downarrow\uparrow\rangle=\langle\downarrow\uparrow|\hat{\mathcal{O}}|\uparrow\downarrow\rangle=e^{-K_z}\sinh K_+\,,\\
&\langle\uparrow\uparrow|\hat{\mathcal{O}}|\downarrow\downarrow\rangle=\langle\downarrow\downarrow|\hat{\mathcal{O}}|\uparrow\uparrow\rangle=e^{K_z}\sinh K_-\,,
\end{aligned} \tag{2·6}$$

where

$$\begin{aligned}
K_z&=(\beta/2m)J_z,\\
K_\pm&=(\beta/2m)(J_x\pm J_y).
\end{aligned} \tag{2·7}$$

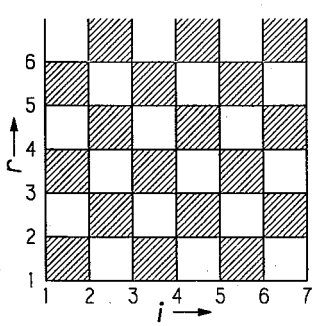

Fig. 1. Graphical representation of the checkerboard decomposition (CBD) in which the equivalent classical lattice is represented by a checkerboard lattice (Ref. 12)); i labels sites on the original 1D lattice and r is a label along the Trotter direction. An Ising spin S_{ir} is assigned to each site (i, r). Only spins on the edges of a shaded square interact with each other. Periodic boundary conditions are imposed along the Trotter direction.

Z_m^{CBD} can be interpreted as the partition function of an Ising model with a checkerboard-like lattice structure; the 2D square lattice is defined in which rows are labeled by $r(1\leqq r\leqq 2m)$ and columns by $i(1\leqq i\leqq N)$ as shown in Fig. 1. Periodic boundary conditions are required in the Trotter direction because of the trace operation. Free chain is assumed in the present study.

The above representation of Z_m^{CBD} offers a very powerful starting formula for numerical studies on quantum statistical mechanics. It is commonly believed[13)] that Monte Carlo simulation is the only means suitable for such calculations. In practice,

Monte Carlo simulations have already been performed on several quantum systems.[3)~5)]

§ 3. The transfer-matrix method

The partition function of the 2D Ising model with the structure shown in Fig. 1 can be computed by using the numerically exact transfer-matrix method.[6),7)] The slightly modified algorithm is as follows: Since we have periodic boundaries along the Trotter direction $S_{i2m+1}=S_{i1}$, the computation is recursively done one column after one along the original chain direction. We retain all 2^{2m} states of the first column $\{S_{1r}\}$ in the storage of the computer. Then we compute the first interaction $\exp[-\beta\mathcal{H}(1,1)]$ between the first and second columns with adding four states of S_{21} and S_{22}. Since we have taken into account all interactions of S_{11} and S_{12} because of free chain, we now perform the trace over S_{11} and S_{12} keeping terms for all states of $\{S_{1r(r\geqq 3)}\}$, S_{21}, S_{22}. Then the second interaction $\exp[-\beta\mathcal{H}(1,3)]$ is considered, and the trace over S_{13} and S_{14} is performed. The remaining interactions are treated in the same way. After completion of the interactions between the first and second columns the trace over all $\{S_{1r}\}$ is completed and all 2^{2m} states of the second column $\{S_{2r}\}$ are retained instead. We may now compute the interactions between the second and third columns and step by step take the trace over the second column $\{S_{2r}\}$. The same procedure is carried out one column after one. Finally the trace is taken over the last column $\{S_{Nr}\}$. In this way we can obtain $Z_m{}^{\mathrm{CBD}}$ numerically for arbitrary temperature T, from which the free energy is given by

$$F^{\mathrm{CBD}}(N,m)=-k_BT\ln Z_m{}^{\mathrm{CBD}} \tag{3·1}$$

Only limitation of the present method is the storage requirement for the factor 2^{2m} which prevents us from studying m larger than $m=10$, while there is much less difficulty to go to larger N.

We use the dimensionless units for the free energy $f=-F/Nk_BT$ and the exchange interaction constant $K=J/k_BT$. In these units we obtain: (1) the internal energy per spin

$$E/J=-\partial f/\partial K\,; \tag{3·2}$$

and (2) the specific heat per spin

$$C/k_B=K^2(\partial^2 f/\partial K^2). \tag{3·3}$$

The temperature dependences of E and C are obtained with good accuracy by computing the free energy for a set of neighboring temperatures and taking the derivatives numerically. In the following the temperature T will be defined in units of J/k_B, the internal energy per spin E in units of J, and the specific heat per spin C in units of k_B.

It should be noted that the case $m=1$ in the above calculation is equivalent to the pair-product approximation of the Heisenberg model which has been solved exactly by Suzuki.[14)]

§ 4. Energy and specific heat calculated in CBD

The free energy $F^{\mathrm{CBD}}(N,m)$ was computed for several values of N and m as a function of T; $N=17, 33, 65, 129, 257$ and $m=1, 2, 4, 5, 6, 7, 8$ for $T\geqq 0.05$. For fixed value

of m the free energy per spin showed no substantial difference between $N=65$ and 129. Therefore we expect that the system with $N \geqq 129$ is large enough to be treated eventually as $N=\infty$ except at extremely low temperatures. The calculated energy and specific heat are presented in conjunction with certain exact and/or very accurate numerical results: (1) the exact solution of Katsura[10] for the XY model; (2) the accurate numerical results of Bonner and Fisher[8] for the ferromagnetic and antiferromagnetic Heisenberg models; and (3) the "experimental data" obtained by means of Monte Carlo simulations by Cullen and Landau.[4] The $m=1$ calculation is also presented because it is equivalent to the pair-product approximation.[14]

(1) *Ferromagnetic Heisenberg model*

Figure 2 shows the results for the energy. The lighter lines are the calculations of $m=2$, 4, 8 with fixed values of $N=129$. The dashed line is the $m=1$ calculation. The bold solid line is the calculation of Bonner and Fisher.[8] Results of the Monte Carlo calculation of Cullen and Landau[4] are also included in Fig. 2. Both results are in a very remarkable agreement, and show a clear progression toward the Bonner and Fisher value at most temperatures as m increases. We note that the low-temperature results benefit from the coincidence that the quantum system and all the classical approximations have the same ground-state energy. Nevertheless, at very low temperatures the quantum effects are poorly reproduced even when $m=8$. The specific-heat results are shown in Fig. 3 which display a nice progression toward the extrapolated Bonner and Fisher curve. They agree fairly well with the Monte Carlo results, although the latter results have the statistics deteriorated as m increases.

(2) *Antiferromagnetic Heisenberg model*

In Fig. 4 are shown the results for the energy, which show a good agreement with the

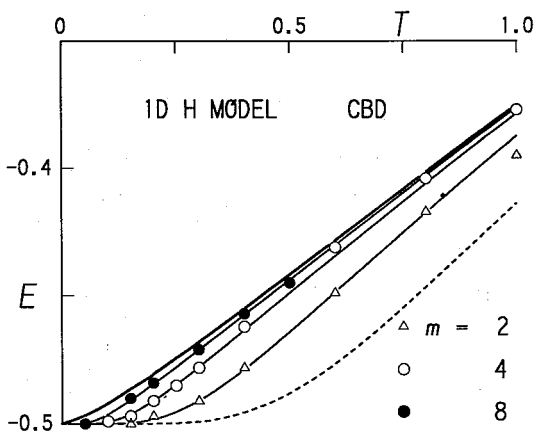

Fig. 2. Temperature dependence of the energy in the 1D ferromagnetic Heisenberg model in CBD. The lighter lines are the calculations of $m=2$, 4, 8. The dashed line is the $m=1$ calculation. The bold solid line is the calculation of Bonner and Fisher (Ref. 8)). Data points are the Monte Carlo results of Cullen and Landau (Ref. 4)).

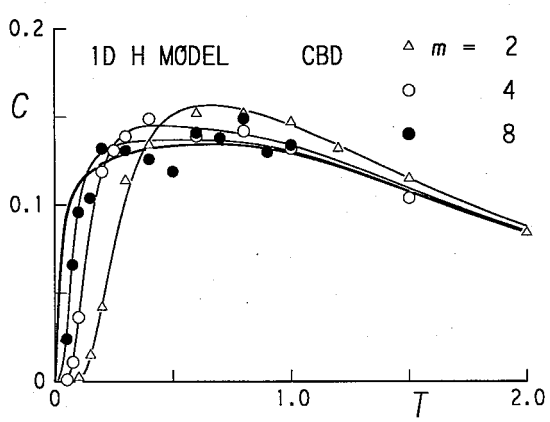

Fig. 3. Specific-heat results for the 1D ferromagnetic Heisenberg model. The lighter lines are the calculations of $m=2$, 4, 8. The bold solid line is the calculation of Bonner and Fisher (Ref. 8)). Data points are the Monte Carlo results of Cullen and Landau (Ref. 4)).

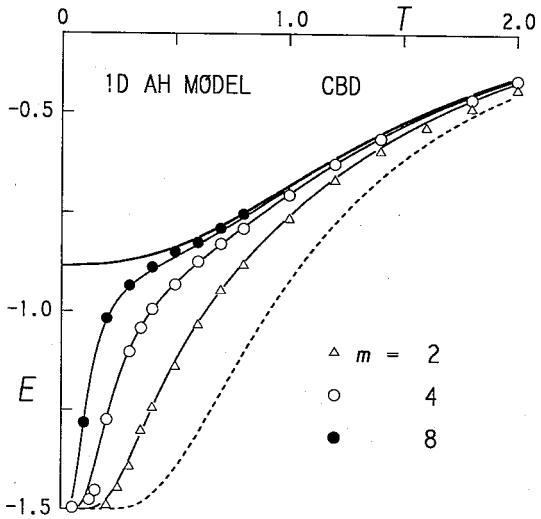

Fig. 4. Temperature dependence of the energy in the 1D antiferromagnetic Heisenberg model in CBD. The lighter lines are the calculations of $m=2$, 4, 8. The dashed line is the $m=1$ calculation. The bold solid line is the calculation of Bonner and Fisher (Ref. 8)). Data points are the Monte Carlo results of Cullen and Landau (Ref. 4)).

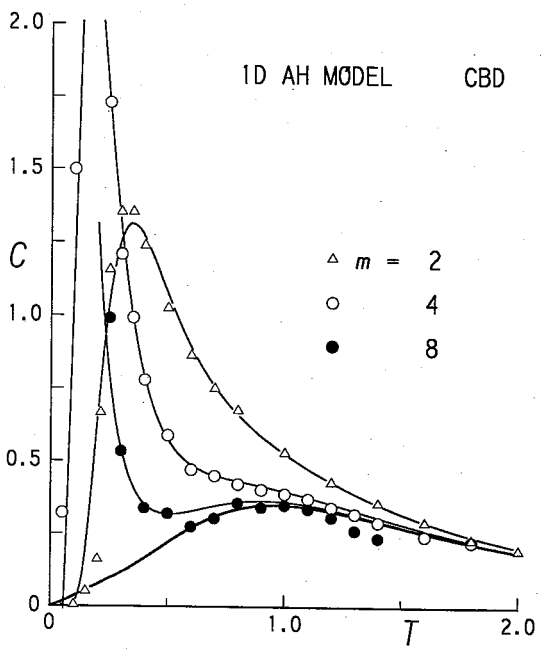

Fig. 5. Specific-heat results for the 1D antiferromagnetic Heisenberg model. The lighter lines are the calculations of $m=2$, 4, 8. The bold solid line is the calculation of Bonner and Fisher (Ref. 8)). Data points are the Monte Carlo results of Cullen and Landau (Ref. 4)).

Monte Carlo results. Both the results show a steady progression toward the Bonner and Fisher value (solid line) with increasing m. The convergence is rapid and the actual estimate is quite good for temperatures $T>0.30$. However, the large difference between the ground-state energy of the quantum system and that of the different classical approximations emphasizes the failure to reproduce the strong quantum effects at extremely low temperatures.

The specific-heat results are displayed in Fig. 5. The progression toward the Bonner and Fisher results (solid line) is quite systematic and for $m=8$ we can see the peak in approximately the correct position. As expected from the energy results, the low-temperature results for the specific heat are poor.

(3) *XY model*

The results for the energy and specific heat are presented in Figs. 6 and 7, and are shown in conjunction with the exact solution of Katsura[10] and with the Monte Carlo results.[4] The general trends observed in the results are very similar to those seen already in the antiferromagnetic Heisenberg model.

(4) *Discussion of the results*

The transfer-matrix method was successfully applied to the calculation of the classical systems equivalent to the 1D quantum Heisenberg and XY models through the Suzuki-Trotter transformation. The classical representation used was the checkerboard

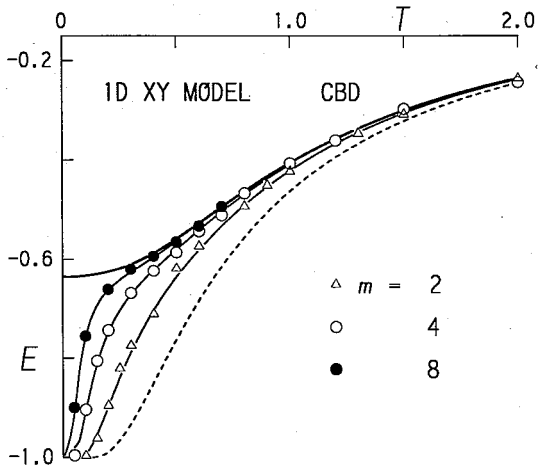

Fig. 6. Temperature dependence of the energy in the 1D XY model in CBD. The lighter lines are the calculations of $m=2$, 4, 8. The dashed line is the $m=1$ calculation. The bold solid line is the exact calculation of Katsura (Ref. 10)). Data points are the Monte Carlo results of Cullen and Landau (Ref. 4)).

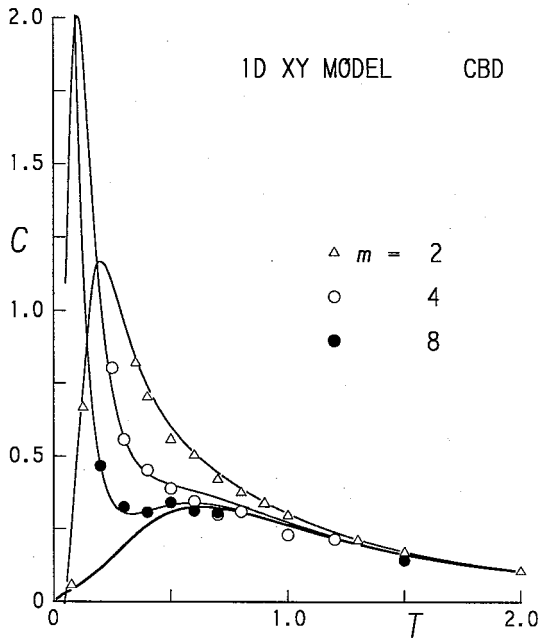

Fig. 7. Specific-heat results for the 1D XY model. The lighter lines are the calculations of $m=2$, 4, 8. The bold solid line is the exact calculation of Katsura (Ref. 10)). Data points are the Monte Carlo results of Cullen and Landau (Ref. 4)).

decomposition (CBD). The energy and specific heat were calculated for a range of the Trotter size from 1 to 8 and over a temperature range from $T=0.05$ to about $T=2.0$. The calculated results showed a remarkable agreement with the Monte Carlo results of Cullen and Landau[4] at every stage of m at all temperatures; the specific-heat results of the latter method have rather poor statistics as m increases while the results of the former are numerically exact. This agreement might be self-evident since both the methods are based on the same classical representation of the free energy.

Good agreement was obtained with the known values of energy and specific heat for moderate value of m so long as the temperature was not too low. Convergence to the correct values as a function of m was quite rapid except in the very-low-temperature region. However, at very low temperatures the convergence of the CBD representation was so poor that the strong quantum efiects were not reproduced up to the Trotter size of $m=8$. The pair-product approximation,[14] which is equivalent to the $m=1$ calculation, was found not to be a good approximation at low temperatures where quantum effects are important.[4]

To overcome this difficulty it is required to select some other classical representations and/or physical quantities which show a rapid convergence. One of the candidates is the RSD representation, the convergence properties of which will be examined in the following sections.

§ 5. The RSD representation

Another classical representation is the real-space decomposition (RSD) introduced by Suzuki.[1] It regards the Hamiltonian as a sum of local two-site parts V_i as given by Eq. (1·3b). Substituting Eq. (1·3b) into Eq. (1·2) and inserting m complete set, the classical representation of the partition function Z_m^{RSD} is given by

$$Z_m^{\mathrm{RSD}}=\mathrm{Tr}[\prod_{i=1}^{N-1}\exp(-\beta V_i/m)]^m \tag{5·1a}$$

$$=\sum_{\alpha_1\alpha_2\cdots\alpha_m}\langle\alpha_1|\prod_{i=1}^{N-1}e^{-\beta V_i/m}|\alpha_2\rangle\langle\alpha_2|\prod_{i=1}^{N-1}e^{-\beta V_i/m}|\alpha_3\rangle\cdots\langle\alpha_m|\prod_{i=1}^{N-1}e^{-\beta V_i/m}|\alpha_1\rangle. \tag{5·1b}$$

Introducing another m complete set as intermediate states and relabeling r sequentially, Eq. (5·1b) is rewritten as

$$Z_m^{\mathrm{RSD}}=\sum_{\alpha_1\alpha_2\cdots\alpha_{2m}}\exp[-\beta\sum_{i=1}^{N-1}\sum_{r\in A'}\tilde{\mathcal{H}}(i,r)], \tag{5·2}$$

where

$$\exp[-\beta\tilde{\mathcal{H}}(i,r)]=\langle S_{ir+1}S_{i+1r}|\exp(-\beta V_i/m)|S_{ir+2}S_{i+1r+1}\rangle. \tag{5·3}$$

The matrix elements (5·3) have the same form as Eq. (2·6). Z_m^{RSD} can be interpreted as the partition function of the 2D Ising model with four spin interactions as shown in Fig. 8. It has been proved mathematically that Z_m^{CBD} transforms into Z_m^{RSD} in the case of free chain.[13] This transformation is easily seen by comparing Figs. 1 and 8. If we relabel r indices in Z_m^{RSD} one column after one as

$$r-1\to r \quad \text{for} \quad i=1 \quad \text{and} \quad r+i-2\to r \quad \text{for} \quad i\geqq 3, \tag{5·4}$$

and use the periodic boundary conditions along the Trotter direction, we find that Z_m^{RSD} transforms into Z_m^{CBD}. Thus both decompositions give the same results for the thermodynamic properties.

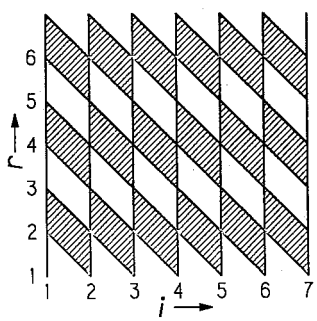

Fig. 8. Graphical representation of the real-space decomposition (RSD) in which the equivalent classical lattice is represented by a skewed checkerboard lattice (Ref. 1)). Each shaded portion indicates a four spin interaction. Periodic boundary conditions are imposed along the Trotter direction.

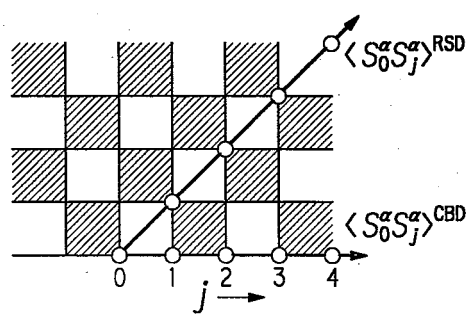

Fig. 9. The interrelation between the correlation functions in CBD and RSD, $\langle S_i^\alpha S_j^\alpha\rangle^{\mathrm{CBD}}$ and $\langle S_i^\alpha S_j^\alpha\rangle^{\mathrm{RSD}}$, respectively. In the 2D lattice for CBD, $\langle S_i^\alpha S_j^\alpha\rangle^{\mathrm{CBD}}$ are defined along the horizontal line while $\langle S_i^\alpha S_j^\alpha\rangle^{\mathrm{RSD}}$ are defined along the diagonal line.

However, the correlation functions $\langle S_i^a S_j^a \rangle (a=x, y, z)$ are not invariant for the transformation mentioned above and therefore the rate of convergence is expected to depend largely on the choice of the decomposition. Figure 9 shows the interrelation between $\langle S_i^a S_j^a \rangle^{\mathrm{CBD}}$ and $\langle S_i^a S_j^a \rangle^{\mathrm{RSD}}$. It should be noted that the CBD destroys the elementary property that the ith spin is to the left of the $(i+1)$th spin.[13]

§ 6. Energy derived from the spin correlation functions

Correlation functions between the center spin at site 0 and spin at site j as displayed in Fig. 9 were calculated numerically exactly by the transfer-matrix method. The algorithm of computation was very similar to the method reported earlier,[7] but slightly modified to calculate the correlations between the center spin specified and any other spins in the 2D lattice. Susceptibilities were obtained from the correlations. Results for the decay behavior of correlations and susceptibilities will be reported in a forthcoming article. The nearest-neighbor correlation is related with the internal energy:

$$E=-2(J_x\langle S_0^x S_1^x\rangle+J_y\langle S_0^y S_1^y\rangle+J_z\langle S_0^z S_1^z\rangle). \tag{6·1}$$

(1) *XY model*

E^{CBD} and E^{RSD}, the energies in RSD and CBD defined by Eq. (6·1), were calculated. Results for E^{RSD} are shown in Fig. 10. The lighter lines are the calculations of $m=2$, 4, 8 for $N=257$, and the dashed lines are for $N=129$. Each calculated energy showed a sudden rise at a temperature T_r on the low-temperature side; T_r decreases as m and N increase. It was found by examining the decay of correlations that an ordering is established below T_r owing to the finiteness of the system. The results for $N=129$ and 257 gave the same numerical results above T_r. Therefore, it may be regarded that the system with $N \geqq 129$ is large enough to be treated eventually as $N=\infty$. The $m=8$

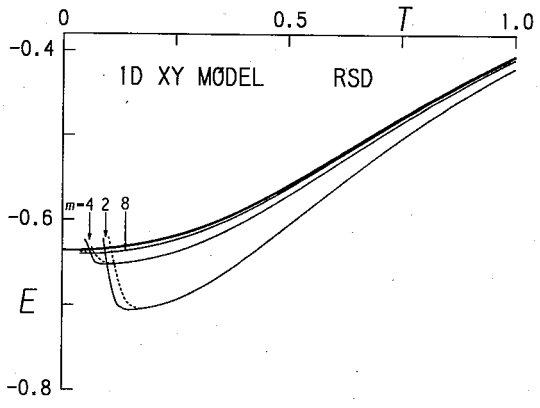

Fig. 10. Temperature dependence of E^{RSD}, the energy derived from the nearest-neighbor correlation in RSD, for the 1D XY model. The lighter solid lines are the calculations of $m=2$, 4, 8 for $N=257$, and the dashed lines are for $N=129$. The bold solid line is the exact calculation of Katsura (Ref. 10)).

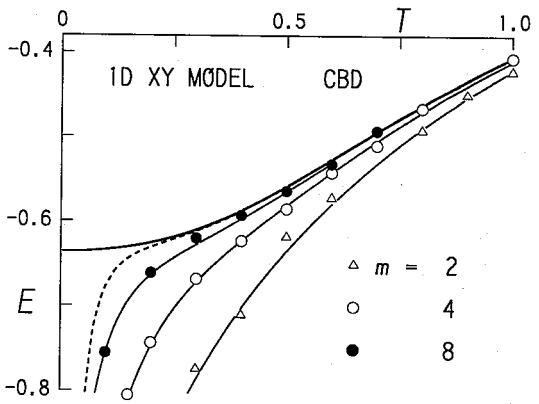

Fig. 11. Temperature dependence of E^{CBD} for the 1D XY model. The lighter lines are the calculations of $m=2$, 4, 8, and the dashed line is the $m\to\infty$ estimation. The bold solid line is the exact calculation of Katsura (Ref. 10)). Data points are the Monte Carlo results of Cullen and Landau (Ref. 4)).

Table I. Energies extrapolated from finite-m calculations. E_{exact} is the exact value of Katsura (Ref. 10)).

T	E_{exact}	E^{RSD}	E^{CBD}
0.0	−0.63662	—	—
0.1	−0.63398	−0.63433	−0.67708
0.15	−0.63060	−0.63077	−0.64405
0.2	−0.62570	−0.62577	−0.63076
0.25	−0.61906	−0.61909	−0.62127
0.3	−0.61049	−0.61050	−0.61159
0.4	−0.58768	−0.58767	−0.58821
0.5	−0.55897	−0.55896	−0.55918

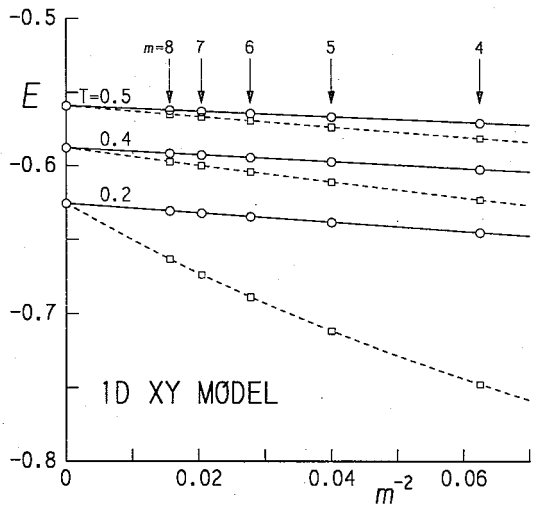

Fig. 12. Energies versus $(1/m)^2$ for the 1D XY model at several temperatures: E^{CBD}(squares) and E^{RSD}(circles).

calculation is very close to the exact calculation of Katsura (bold solid line) all over the temperature range studied; $T_r < 0.05$ for $N=129$ and 257.*) Results for E^{CBD} are shown in Fig. 11. It was found that E^{CBD} coincides with that derived from the free energy F^{CBD}. By comparing E^{RSD} with E^{CBD} at every stage of m, it is clearly seen that E^{RSD} converges much faster than E^{CBD}.

In Fig. 12 the energies E^{RSD} and E^{CBD} are plotted versus $(1/m)^2$. It is evident that the same limiting energy is approached linearly with $(1/m)^2$ but the convergence rate of CBD is much slower at low temperatures than RSD; at $T=0.2$ E^{CBD} deviates markedly from the linear relation with $(1/m)^2$ suggesting the need to include higher order corrections. A relation of the form:

$$E(m)=E(\infty)+a/m^2 \qquad (6\cdot2)$$

holds quite accurately for RSD; the same relation holds for CBD but less accurately at low temperatures because of slow convergence. The limiting energies are tabulated in Table I; these values are extrapolated from $m=5, 6, 7, 8$ for RSD, and from $m=6, 7, 8$ for CBD at low temperatures. The limiting energy in CBD is included in Fig. 11 (dashed line). The agreement with the exact value is very excellent for RSD, which indicates that the strong quantum effects at very low temperatures are well reproduced by E^{RSD}. However, the agreement is somewhat worse for CBD. This poor convergence of the correlation functions in CBD arises from the fact that this type of decomposition destroys the

*) The values of T_r presented in Fig. 10 are different from those presented in Fig. 5 of Ref. 11). This is because that the XZ model was used in the preliminary work and the energy was obtained from $\langle S_0^z S_1^z\rangle$ by assuming the rotational symmetry; $\langle S_0^x S_1^x\rangle = \langle S_0^z S_1^z\rangle$. In the present work the XY model was used and the energy was obtained directly from $\langle S_0^x S_1^x\rangle$ and $\langle S_0^y S_1^y\rangle$. Both models gave the same numerical values above T_r although the values of T_r were dependent on the model.

elementary property that the ith spin is to the left of the $(i+1)$th spin.[13]

The extrapolation formula (6·2) is seen to be complementary to the finite-chain extrapolation of Bonner and Fisher;[8] the properties of infinite chain can be estimated from those of finite chains by using a relation of the form:

$$E(N)=E(\infty)+\beta/N^2 . \tag{6·3}$$

Their numerical method is to diagonalize the full Hamiltonian for finite chains, which corresponds to $m=\infty$. This complementarity reflects the fact that the matrix elements (2·6) are symmetrical with respect to i and r. Recently Suzuki[15] has proved rigorously that the convergence rate of the classical representations is proportional to $(1/m)^2$.

The specific heat was obtained by differentiating E^{RSD} numerically with respect to T. The results are shown in Fig. 13. As expected from the energy results, they show a rapid convergence to the exact solution of Katsura (solid line). The limiting value extrapolated by use of Eq. (6·2) agrees with the exact solution.

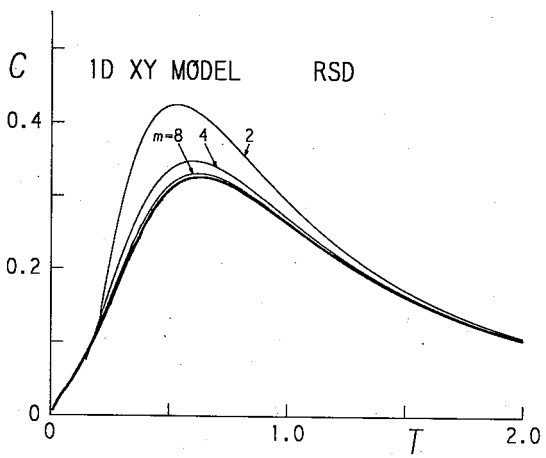

Fig. 13. Results for specific heat derived from E^{RSD} for the 1D XY model. The lighter lines are the calculations of $m=2$, 4, 8. The bold solid line is the exact calculation of Katsura (Ref. 10)).

(2) *Heisenberg models*

The results for the energy and specific heat of the ferromagnetic and antiferromagnetic Heisenberg models are presented in Figs. 14~17. They are shown in conjunction with the Bonner and Fisher value (solid line). The general trends observed in the results are very similar to those seen already in the XY model. The limiting values agree with the Bonner and Fisher results precisely in

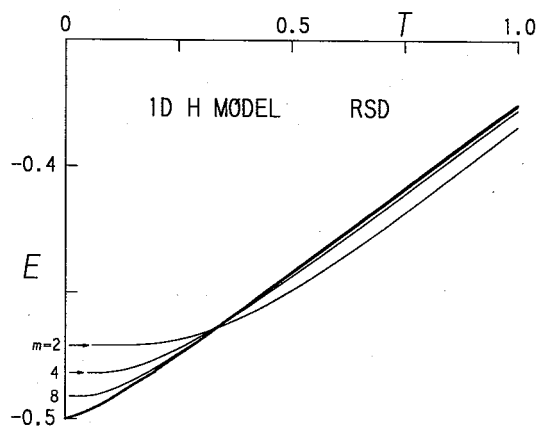

Fig. 14. Temperature dependence of E^{RSD} for the 1D ferromagnetic Heisenberg model. The lighter lines are the calculations of $m=2$, 4, 8. The bold solid line is the calculation of Bonner and Fisher (Ref. 8)).

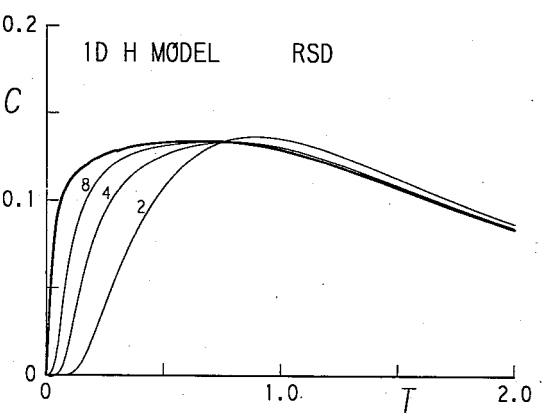

Fig. 15. Results for specific heat derived from E^{RSD} for the 1D ferromagnetic Heisenberg model. The lighter lines are the calculations of $m=2$, 4, 8. The bold solid line is the calculation of Bonner and Fisher (Ref. 8)).

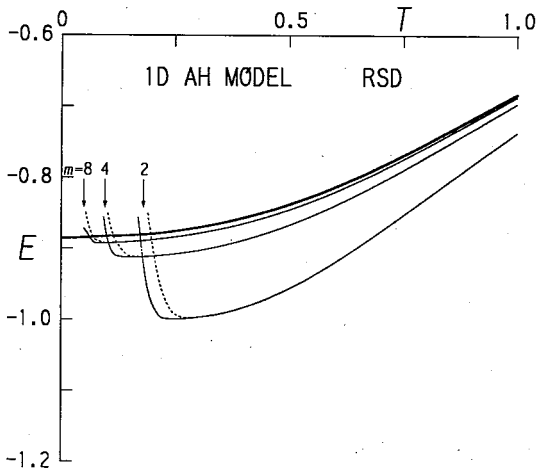

Fig. 16. Temperature dependence of E^{RSD} for the 1D antiferromagnetic Heisenberg model. The lighter solid lines are the calculations of $m=2$, 4, 8 for $N=257$, and the dashed lines are for $N=129$. The bold solid line is the calculation of Bonner and Fisher (Ref. 8)).

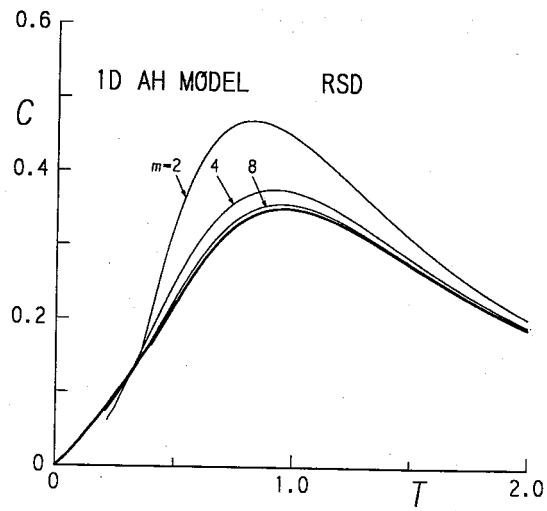

Fig. 17. Results for specific heat derived from E^{RSD} for the 1D antiferromagnetic Heisenberg model. The lighter lines are the calculations of $m=2$, 4, 8. The bold solid line is the calculation of Bonner and Fisher (Ref. 8)).

these cases.

(3) *Discussion of the results*

The spin correlation functions of the 1D Heisenberg and XY models were calculated by applying the transfer-matrix method to the equivalent classical systems in the RSD and CBD representations. The energy was defined in terms of the nearest-neighbor correlation; E^{RSD} and E^{CBD}. E^{RSD} was found to converge much faster than E^{CBD}, while E^{CBD} agreed with the energy derived from the free energy. Convergence of E^{RSD} as a function of m was quite rapid and showed the $(1/m)^2$ dependence except extremely-low-temperature region. The $m\to\infty$ behavior was estimated accurately. The limiting values were agreed with the correct values excellently.

The rapid convergence of E^{RSD} as well as the presence of the extrapolation scheme confirms the surmise of Suzuki et al.[3] that satisfactory numerical estimates for thermodynamic quantities could be obtained for moderate value of m.

§ 7. Summary and conclusions

The transfer-matrix method has been used to study the 2D Ising models equivalent to the 1D quantum spin systems through the Suzuki-Trotter transformation. Convergence properties have been examined in two different representations; checkerboard decomposition (CBD) and real-space decomposition (RSD). The rates of convergence of the thermodynamic quantities are the same in the both representations. Nevertheless, the spin correlation functions in RSD converge much faster than those in CBD. This is because the elementary property is destroyed in CBD that the ith spin is to the left of the $(i+1)$th spin. The $m\to\infty$ behavior can be estimated accurately from a new type of extrapolation scheme which is complementary to the finite-chain extrapolation of Bonner

and Fisher;[8] the results extrapolated from finite Trotter size are as exact as those extrapolated from finite chains.

In conclusion, the present study has realized the hope of Suzuki et al.[3] that good numerical estimates could be obtained from the calculations with moderate value of m. The basic reason for the success has been the selection of the classical representation and thermodynamic quantity which show a rapid convergence in actual application of the Suzuki-Trotter formula. It is to be hoped that the information obtained from the present study provides meaningful guide for constructing a particular Monte Carlo algorithm to perform simulations on more complicated quantum systems. The present method can be applied with slight modifications to other 1D quantum system, such as fermion lattice model and Hubbard model. The results will appear in the near future.

Acknowledgements

The author would like to thank Professor M. Suzuki for stimulating discussion and for sending the author his papers prior to publication, and Mr. T. Yokota for useful discussion. The author is grateful for the assistance of members of the computer center of JAERI.

References

1) M. Suzuki, Prog. Theor. Phys. **56** (1976), 1454.
2) H. F. Trotter, Proc. Amer. Math. Soc. **10** (1959), 545.
M. Suzuki, Commun. Math. Phys. **51** (1976), 183.
3) M. Suzuki, S. Miyashita and A. Kuroda, Prog. Theor. Phys. **58** (1977), 1377.
4) J. J. Cullen and D. P. Landau, Phys. Rev. **B27** (1983), 297.
5) H. De Raedt and A. Lagendijk, preprint, (to be published in Rev. Mod. Phys.) and references therein.
6) I. Morgenstern and K. Binder, Phys. Rev. **B22** (1980), 288.
7) H. Betsuyaku, J. Phys. Soc. Jpn. Suppl. **52** (1983), 225.
8) J. C. Bonner and M. E. Fisher, Phys. Rev. **135** (1964), A640.
9) E. Lieb, T. Schultz and D. Mattis, Ann. of Phys. **16** (1961), 407.
10) S. Katsura, Phys. Rev. **127** (1962), B1508.
11) H. Betsuyaku, Phys. Rev. Lett. **53** (1984), 629.
12) M. Barma and B. S. Shastry, Phys. Rev. **B18** (1978), 3351.
13) H. De Raedt, A. Lagendijk and J. Fivez, Z. Phys. **B46** (1982), 261.
14) M. Suzuki, J. Phys. Soc. Jpn. **21** (1966), 2274.
15) M. Suzuki, Phys. Rev. **B31** (1985), No. 5; J. Math. Phys. (1985), March.